ISSN 0967-0912, Steel in Translation, 2016, Vol. 46, No. 11, pp. 781–787. © Allerton Press, Inc., 2016.
Original Russian Text © N.A. Kozyrev, N.V. Kibko, A.A. Umanskii, D.A. Titov, L.P. Bashchenko, 2016, published in Izvestiya Vysshikh Uchebnykh Zavedenii, Chernaya Metallurgiya, 2016, No. 11, pp. 806–813.

Composition of C–Si–Mn–Cr–W–V Powder Wire and Quality of Surfacing

N. A. Kozyrev*, N. V. Kibko, A. A. Umanskii***, D. A. Titov****, and L. P. Bashchenko*******

Siberian State Industrial University, Novokuznetsk, Russia

**e-mail: Kozyrev_na@mtsp.sibsiu.ru*

***e-mail: krivicheva_nv@mail.ru*

****e-mail: umanskii@bk.ru*

*****e-mail: titov.dima@mail.ru*

******e-mail: luda.baschenko@gmail.com*

Received January 13, 2016

Abstract—The influence of the composition of powder wire on the properties of the applied layer on steel samples is studied in the laboratory. If amorphous graphite in 35V9Kh3SF powder wire is replaced by material containing carbon and fluorine, the porosity of the applied layer is reduced, and fewer nonmetallic inclusions (including row oxide inclusions and undeformable silicates) are present. Statistical analysis of the experimental data illustrates the influence of the carbon equivalent of the 35V9Kh3SF powder wire on the hardness of the applied layer (including the mean surface hardness and the microhardness of martensite). With increase in the carbon equivalent calculated by the Paton Institute's formula, the hardness of the applied layer linearly increases.

Keywords: hardening, powder wire, thermal durability, surfacing, rollers, microstructure, nonmetallic oxide inclusions, porosity

DOI: 10.3103/S0967091216110073

To strengthen the rollers in hot-rolling mills, PP-Np-35V9Kh3SF wire (corresponding to State Standard GOST 26101–84) is widely used at present [1–5]. The applied metal has high wear resistance at high temperatures. However, its thermal stability is relatively low. Therefore, the rollers fail with considerable frequency [6–9].

The thermal stability of rollers surfaced with PP-Np-35V9Kh3SF wire (70 rolling cycles) is about a third of that for 25Kh5FMS wire (200 cycles), according to the data in [10].

Accordingly, research is underway to improve the composition of C–Si–Mn–Cr–W–V powder wire. For example, OOO TM.BELTEK has developed BELTEK-N500RM, BELTEK-N505RM, and BELTEK-N550RM powder wire, capable of improving both the crack resistance and wear resistance [10]. The best performance is obtained for BELTEK-N505RM wire: the improvements in crack resistance and wear resistance are better than those for PP-Np-35V9Kh3SF wire by factors of 2 and 1.3, respectively. The structure of the metal applied by means of BELTEK-N505RM wire consists of troostite and martensite with thin austenite borders along the grain boundaries. A few inclusions of carbide eutectic are also seen along the grain boundaries [10].

We now determine the influence of the composition of C–Si–Mn–Cr–W–V powder wire on the properties of the surfaced rollers [11]. In the laboratory, samples of powder wire with dust containing carbon and fluorine (metallurgical waste) are prepared. The composition of the samples (by mass) is as follows

21–46% Al_2O_3; 18–27% F; 8–15% Na_2O;
0.4–6.0% K_2O; 0.7–2.3% CaO; 0.5–2.5% SiO_2;
2.1–3.3% Fe_2O_3; 12.5–30.2% C_{tot};
0.07–0.90% MnO; 0.06–0.90% MgO;
0.09–0.19% S; 0.10–0.18% P.

The dust containing carbon and fluorine is introduced instead of amorphous graphite, with allowance for the fact that the carbon in the dust is of greater activity and reduces oxides in the metal and slag (with the formation of carbon oxides) [12, 13]. Nickel is introduced in some of the samples. Two batches of samples are manufactured. In the first batch, we add 0.29, 0.33, and 0.61% of nickel to the amorphous carbon and the dust containing carbon and fluorine (samples *3–5*, respectively, in the table). In the second batch, we add 0.38, 0.46, and 0.58% of nickel to the amorphous graphite and the dust containing carbon and fluorine (samples *8–10*, respectively, in the table).The

Chemical composition of the samples

Sample	Content, %										
	C	Si	Mn	Cu	Cr	Mo	Ni	Al	W	V	Ti
1	0.27	1.62	1.42	0.19	2.93	0.14	0.14	0.004	11.39	0.47	0.020
2	0.23	0.69	1.04	0.21	1.92	0.09	0.16	0.039	5.58	0.15	0.019
3	0.24	0.83	1.83	0.24	2.16	0.09	0.29	0.054	7.49	0.27	0.019
4	0.26	0.77	1.72	0.26	2.17	0.09	0.33	0.042	6.12	0.29	0.016
5	0.33	1.37	1.06	0.22	2.80	0.10	0.61	0.070	10.71	0.42	0.040
6	0.14	0.45	1.69	0.02	2.60	0.01	0.08	0.019	8.84	0.36	0.005
7	0.14	0.51	1.73	0.11	2.09	0.01	0.08	0.012	7.66	0.14	0.005
8	0.13	0.45	1.74	0.09	2.18	0.01	0.38	0.008	8.11	0.09	0.005
9	0.13	0.49	1.68	0.09	2.27	0.01	0.46	0.005	8.21	0.13	0.004
10	0.13	0.60	1.54	0.09	2.66	0.02	0.58	0.044	7.58	0.15	0.005

Samples *1* and *6* contain amorphous graphite. Samples *2* and *7* contain added carbon–fluorine dust. Samples *3–5* and *8–10* contain added carbon–fluorine dust and nickel.

concentrations of silicon, manganese, molybdenum, tungsten, and vanadium are modified here.

The chemical composition of the applied metal is determined by an X-ray fluorescent method on an XRF-1800 spectrometer and by an atomic-emission method on a DFS-71 spectrometer.

After surface etching in 4% nitric-acid solution, the samples undergo metallographic analysis by means of an Olympus GX-51 optical microscope (magnification range 100–1000). The grain size is determined in accordance with State Standard GOST 5639–82 (at a magnification of 100). The martensite score is assessed by comparing the structure with standards corresponding to the dimensions of the martensite needles in Table 6 of State Standard GOST 8233–56. The length of the martensite needles is determined by means of SIAMS Photolab-700 metallographic software. The process of nonmetallic inclusions in longitudinal samples of the applied layer is investigated in accordance with State Standard GOST 1778–70. The polished surface is studied by means of a LaboMet-1I metallographic microscope (magnification 100).

The hardness is determined by the Rockwell and Vickers methods. The Rockwell hardness is measured in accordance with State Standard GOST 9013–59. The properties of the martensite are investigated by determining the Vickers microhardness of the structural components in accordance with State Standard GOST 9450–76. We use an HVS-1000 digital instrument with automatic rotation of the head and digital data display. For each sample, the microhardness of the martensite is measured ten times, as follows: a probe in the form of a tetrahedral diamond pyramid is pressed into the surface of a preliminarily etched metallographic section. The load is 1 N. After removing the load, the hardness is determined in accordance with the length of the diagonals in the impressions obtained. Automatic calculation of the Vickers hardness and storage of the image with the impression is ensured by connecting a CCD camera to a computer with a video card and image-analysis software.

Metallographic analysis of samples obtained with the addition of amorphous graphite shows that they consist of martensite with residual austenite in the interaxial region (Figs. 1a and 1b).

Sample *1* (from the first batch) has dendritic structure. Point defects of tungsten and chromium carbides are distributed throughout the grains (Fig. 1a).

Sample *6* (second batch) contains coarse martensite needles (score 10), a small quantity of residual austenite, and point carbides (Fig. 1b). The grain size corresponds to scores of 6 and 7 (Fig. 2). Pores are seen over the whole surface of the section (pore size 640–1077 μm).

The use of carbon–fluorine dust in place of amorphous graphite reduces the porosity, as we see if we compare sample *6* (with amorphous graphite) and sample *7* (with carbon–fluorine dust). The microstructure is different: besides large martensite needles (score 10) and a small quantity of residual austenite, sample *7* contains ferrite as an individual structural component (and, in some regions, as a grid), as well as disperse carbides (Fig. 1f). Thus, the addition of carbon–fluorine dust facilitates the appearance of ferrite, with grain-size scores of 5 and 4 (Fig. 2).

On account of the introduction of carbon–fluorine dust, sample *2* contains troostite needles and a few thin austenite borders at the grain boundaries, as well as a small quantity of disperse carbide inclusions.

The introduction of 0.29, 0.33, and 0.61% Ni in the wire does not affect the microstructure of the applied layer. Samples *3–5* have similar structure to sample *2*: troostite needles with martensite and residual austenite, as well as a small quantity of disperse carbide inclusions (Figs. 1b–1d).

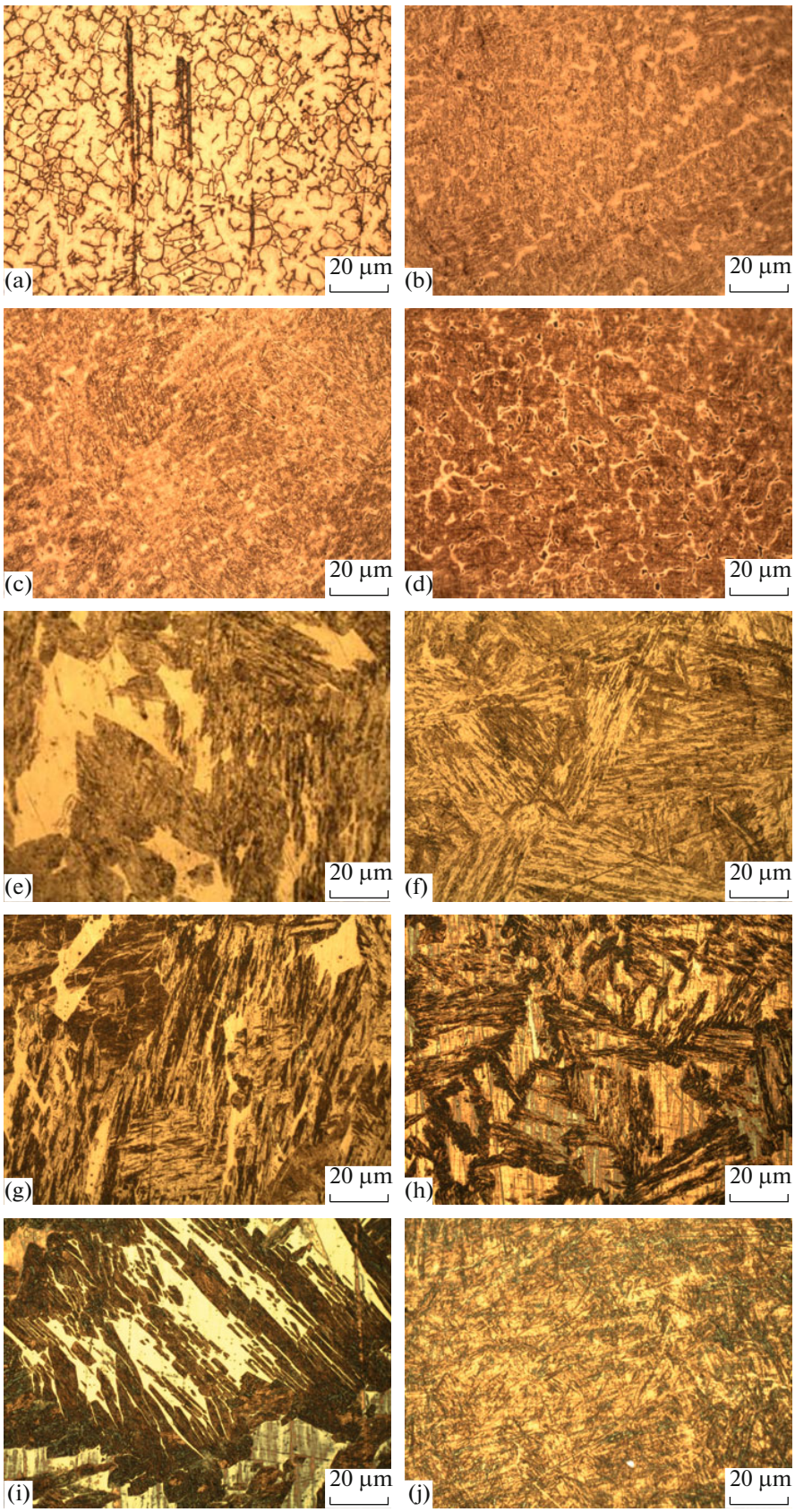

Fig. 1. Microstructure of samples *1* (a), *3* (b), *4* (c), *5* (d), *6* (e), *7* (f), *8* (g), *9* (h, i), and *10* (j).

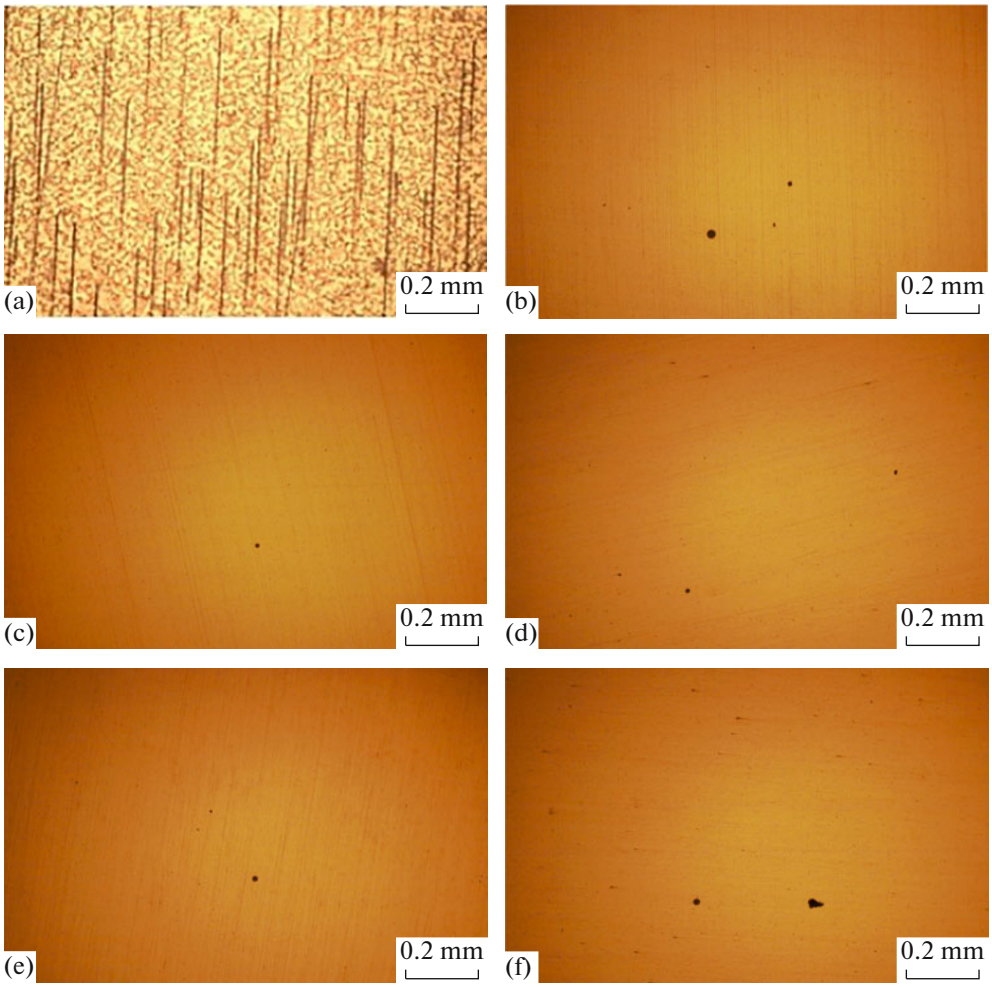

Fig. 2. Nonmetallic inclusions in samples *1* (a), *6* (b), *7* (c), *8* (d), 9 (e), and *10* (f).

Adding 0.38 and 0.46% Ni to the batch (samples *8* and *9*) also has practically no effect on the structure of the 35V9Kh3SF steel produced. The samples contain large martensite needles (score 10), with ferrite as an individual structural component and a small quantity of residual austenite. We also note a small quantity of disperse carbide inclusions (Figs. 1g and 1i). The austenite grain size corresponds to scores of 5–7 for sample *8* and scores of 5 and 6 for sample *9* (Fig. 2).

The introduction of more nickel (0.58%) in the wire (sample *10*) eliminates the ferrite component. The structure consists of large martensite needles (score 10), as well as a small quantity of residual austenite with a grain-size score of 6 and 7 (Fig. 2). Point carbide inclusions are also present (Fig. 1j). The martensite is more disperse than in the other samples: the martensite needles measure 7–42 μm. In that case, the porosity is reduced.

In samples containing amorphous graphite, we note a considerable quantity of oxygen row inclusions (Fig. 2a); these are stress concentrators and give rise to large cracks. We also observe point oxide inclusions (score 2a and 1a) and undeformable silicates (score 1a), as shown in Fig. 2b.

The introduction of carbon–fluorine dust in the batch in place of amorphous graphite reduces the content of nonmetallic inclusions; ensures the removal of a considerable quantity of oxygen row inclusions (samples of the first batch); and also eliminates the undeformable silicates and reduces the content of point oxide inclusions from a score of 2a to 1a (samples of the second batch), as seen in Fig. 2c.

The changes in microstructure on introducing carbon–fluorine dust and nickel in the batch are accompanied by changes in the property of the applied layer. Note that the carbon equivalent C_e has a considerable influence on the properties of 35V9Kh3SF steel. Accordingly, we determine C_e (%) for the samples on the basis of three different formulas: that proposed by

the International Institute of Welding (European standard EN 1011-2:2001)

$$C_e = C + \frac{Mn}{6} + \frac{Cr + Mo + V}{5} + \frac{Cu + Ni}{15}; \quad (1)$$

the formula proposed by the Paton Electrowelding Institute

$$C_e = C + \frac{Si}{24} + \frac{Mn}{6} + \frac{Cr}{5} + \frac{Mo}{4} + \frac{Ni}{10} + \frac{V + Cu}{14}; \quad (2)$$

and the formula in State Standard GOST 27772–88 [14, 15]

$$C_e = C + \frac{Si}{24} + \frac{Mn}{6} + \frac{Cr}{5} + \frac{Mo}{4} + \frac{Ni}{40} + \frac{Cu}{13} + \frac{V}{14} + \frac{P}{2}. \quad (3)$$

Here C, Si, Mn, Cr, Mo, V, V, Cu, Ni, and P denote the concentrations of the corresponding elements, %.

According to these three formulas, the values of the carbon equivalent for the samples of 35V9Kh3SF powder wire are as follows:

Sample	C_{e1}	C_{e2}	C_{e3}
1	1.23	1.25	1.24
2	0.85	0.88	0.86
3	1.08	1.09	1.07
4	1.09	1.10	1.08
5	1.23	1.25	1.21
6	1.02	0.99	0.99
7	0.89	0.89	0.89
8	0.90	0.92	0.90
9	0.92	0.94	0.91
10	0.99	1.02	0.98

The hardness of the applied layer when using 35V9Kh3SF powder wire is as follows (mean/minimum/maximum):

Sample	*HRC*
1	49.0/48.7/49.2
2	50.8/49.3/51.2
3	53.3/51.0/54.0
4	53.0/51.0/53.5
5	54.8/53.4/55.1
6	45.5/45.2/46.0
7	46.0/45.2/47.0
8	45.5/45.2/47.0
9	47.2/45.0/49.0
10	48.0/46.5/50.0

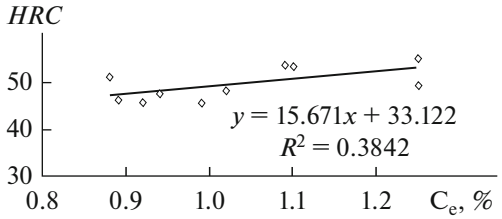

Fig. 3. Dependence of the hardness of the applied layer on the carbon equivalent of the 35V9Kh3SF powder wire employed.

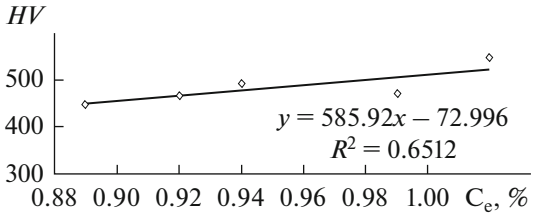

Fig. 4. Dependence of the microhardness of the martensite in the applied layer on the carbon equivalent of the 35V9Kh3SF powder wire employed.

The microhardness μ_H of the martensite in the applied layer when using 35V9Kh3SF powder wire and the wear rate of the applied layer are as follows:

Sample	μ_H, *HV*	Wear rate, g/turn
6	471	0.00088
7	449	0.00052
8	464	0.00052
9	493	0.00065
10	547	0.00068

The results for the hardness of the applied layer, the microhardness of the martensite, and the wear rate of the applied layer indicate that the carbon equivalent has a significant influence on the hardness. With increase in carbon equivalent of the 35V9Kh3SF powder wire, we note increase in both the mean hardness of the applied layer (Fig. 3) and the microhardness of the martensite in that layer (Fig. 4). The Paton Institute's formula is used in plotting Figs. 3 and 4, since it results in the best reliability of the results.

In Fig. 5, we show the indenter impressions in determining the microhardness.

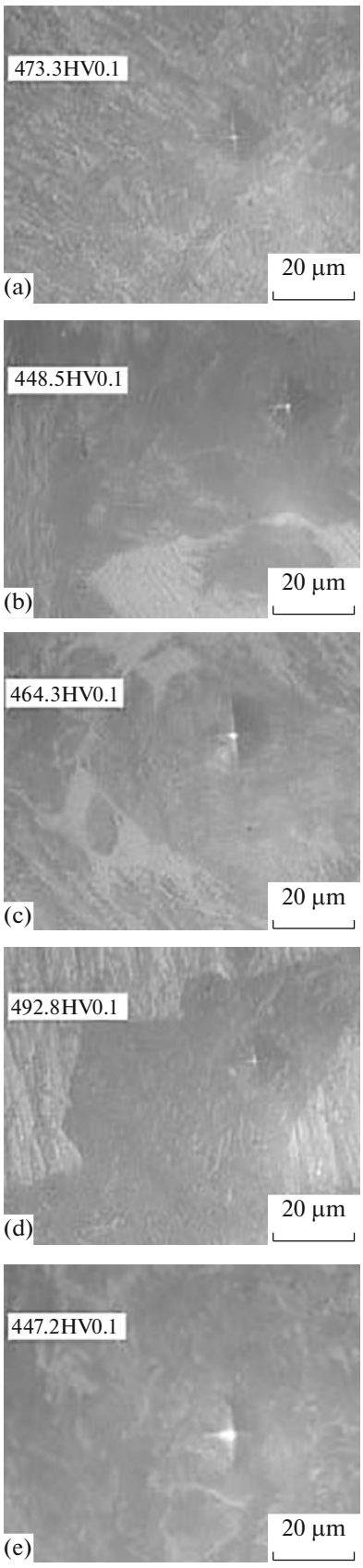

Fig. 5. Indenter impressions in determining the microhardness of the martensite in the applied layer for samples *6* (a), *7* (b), *8* (c), *9* (d), and *10* (e).

CONCLUSIONS

Introducing dust containing carbon and fluorine (metallurgical waste) in 35V9Kh3SF powder wire instead of amorphous graphite reduces the porosity of the applied layer and also the content of nonmetallic inclusions (including row oxide inclusions and undeformable silicates).

Statistical analysis of the experimental data illustrates the influence of the carbon equivalent of the 35V9Kh3SF powder wire on the hardness of the applied layer (including the mean surface hardness and the microhardness of martensite).

ACKNOWLEDGMENTS

Financial support was provided by the Russian Ministry of Education and Science (project 11.1531.2014/k). Equipment from the Collective Use Center at Siberian State Industrial University was used in the research.

REFERENCES

1. Traino, A.I., Rational roller operation and restoration, *Steel Transl.*, 2008, vol. 38, no. 10, pp. 871–875.
2. Shebanits, E.N., Omel'yanenko, N.I., Kurakin, Yu.N., Matvienko, V.N., Leshchinskii, L.K., Dubinskii, B.E., and Stepnov, K.K., Improving the fracture toughness and wear resistance of hardfaced hot-rolling-mill rolls, *Metallurgist*, 2012, vol. 56, nos. 7–8, pp. 613–617.
3. Danilov, L.I., Skorokhvatov, N.B., and Sobolev, V.F., Increase of service life of counter rollers of 2000 rolling mill of hot strip rolling in Severstal Company, *Chern. Metall.*, 2004, no. 8, pp. 68, 69.
4. Ogarkov, N.N. and Belyaev, A.I., *Stoikost' i kachestvo prokatnykh valkov (Durability and Quality of Rolling Mills), Magnitogorsk*: Magnitogorsk. Gos. Tekh. Univ., 2008.
5. Matvienko, V.N., Gulakov, S.V., and Royanov, V.A., Reduction by welding of metallurgical equipment parts in the conditions of Il'ich Magnitogorsk Metallurgical Plant, *Met. Lit'e Ukr.*, 2005, nos. 7–8, pp. 66–69.
6. Gulidov, I.N., *Oborudovanie prokatnykh tsekhov: ekspluatatsiya i nadezhnost' (Equipment of Rolling-Mill Shops: Operation and Reliability)*, Moscow: Intermet Inzhiniring, 2004.
7. Ryabtsev, I.A. and Kondrat'ev, I.A., *Mekhanizirovannaya elektrodugovaya naplavka detalei metallurgicheskogo oborudovaniya (Automated Electric-Arc Welding of Metallurgical Equipment Parts)*, Kiev: Ekotekhnologiya, 1999.
8. Kal'yanov, V.N. and Novitskaya, A.V., Increase of durability of rolling mills when welding by economically alloyed steel, *Svar. Proizvod.*, 1997, no. 10, pp. 23–27.
9. Kondrat'ev, I.A., Ryabtsev, I.A., and Kuskov, Yu.M., Arc and electroslag welding of rollers of rolling mills, *Svarshchik*, 2004, no. 1, pp. 7–9.
10. Titarenko, V.I., Golyakevich, A.A., Orlov, L.N., Mosypan, V.V., Babenko, M.A., Telyuk, D.V., and

Tarasenko, V.V., Reducing welding of rollers of rolling mills with flux-cored wire, *Svar. Proizvod.*, 2013, no. 7, pp. 29–32.

11. Kozyrev, N.A., Titov, D.A., Starovatskaya, S.N., Shurupov, V.M., and Goryushkin, V.F., The influence of the introduction of the charge flux-cored wire system with C–Si–Mn–Cr–W–V carbonfluorine-containing additives and nickel, *Izv. Vyssh. Uchebn. Zaved., Chern. Metall.*, 2014, no. 6, pp. 31–33.
12. Kozyrev, N.A., Kryukov, R.E., Roor, A.V., Bashchenko, L.P., and Lipatova, U.I., Research and development of new carbon-fluorine-containing additives for welding fluxes, *Izv. Vyssh. Uchebn. Zaved., Chern. Metall.*, 2015, vol. 58, no. 4, pp. 258–261.
13. Kozyrev, N.A., Kryukov, N.E., Kryukov, R.E., Igushev, V.F., and Koval'skiy, I.N., Technological aspects of using a carbon–fluorine-containing addition in submerged-arc welding, *Welding Int.*, 2016, vol. 30, no. 4, pp. 325–328.
14. Makarov, E.L. and Yakushin, B.F., *Teoriya svarivaemosti stalei i splavov (Theory of Welding Characteristics of Steels and Alloys)*, Moscow: Mosk. Gos. Tekh. Univ. im. N.E. Baumana, 2014.
15. Lakhtin, Yu.M. and Leont'eva, V.P., *Materialovedenie (Material Science)*, Moscow: Al'yans, 2013.

Translated by Bernard Gilbert